VI International Conference on Computational Methods for Coupled Problems in Science and Engineering
COUPLED PROBLEMS 2015
B. Schrefler, E. Oñate and M. Papadrakakis (Eds)

A RBF-BASED LOCAL COLLOCATION METHOD FOR MODELLING THERMOMECHANICAL PHENOMENA DURING DC CASTING OF ALUMINIUM BILLETS

BOŠTJAN MAVRIČ[*] AND BOŽIDAR ŠARLER[*,†]

[*]Laboratory for Simulation of Materials and Processes
Institute of Metals and Technology
Lepi pot 11, SI-1000 Ljubljana, Slovenia
e-mail: bostjan.mavric@imt.si

[†] Laboratory for Multiphase Processes
University of Nova Gorica
Vipavska 13, SI-5000 Nova Gorica, Slovenia
e-mail: bozidar.sarler@ung.si

Key words: meshless methods, local radial basis function collocation method, multiquadrics, thermoelasticity, direct-chill casting.

Abstract. In this work, the local radial basis function collocation method is applied to the thermoelasticity with intention to model the low-frequency electromagnetic direct-chill casting process of aluminium billets. The devised thermoelastic model is coupled with the heat transport model for the DC casting process and preliminary results on the stress state are presented. The effect of the casting speed and the application of the electromagnetic field on the principal stresses is presented.

1 INTRODUCTION

The thermomechanical phenomena that occur during DC casting of aluminium billets can have significant impact on the quality of the cast piece. Under specific stress conditions hot tearing and cracking of the cast piece can occur [1, 2]. Unwanted large deformations of the cast piece lead to its scrapping. The deformations also drastically influence the heat transfer efficiency at the contact with the mold, which can lead to unwanted remelting and melt outbreaks.

Modelling of thermomechanical phenomena during this process is not an easy task. In addition to elastic deformation, the strain field also has contributions from viscoplastic creep, plastic deformation, and thermal expansion. All these phenomena occur in nonhomogeneous material with strong dependence of material properties on the temperature. The importance of the stresses during the DC casting process results in a large number of papers dealing with its predictive modelling. The first simple models were developed quite early [3, 4] and consider heat diffusion and thermomechanics by simple constitutive relations. At present, more sophisticated models, involving constitutive relations coupled with heat and fluid flow are being developed [1, 5].

Recently, the performance of the DC casting process is being upgraded by the application

of the oscillating electromagnetic field, with intention of improving the quality of the casting by stirring the melt [6]. To better understand the process, the numerical models are developed in parallel with industrial applications [7, 8].

Many models describing the DC casting process already exist [1, 5, 9, 10] and can provide accurate results. Existing models mainly employ the Finite Element Method (FEM), which may prove inefficient in some circumstances. The local meshless method used in our work has several advantages over FEM [11, 12]. There is no need for expensive polygonization of the domain, since the only information needed are the positions of the points. The computational points can be easily added or removed to achieve optimal accuracy [13] and complex geometries can be easily described since irregular node arrangements can be used. The local radial basis function collocation method (LRBFCM) has already been successfully applied to many physical and engineering problems: heat and fluid flow with [14] and without [15] the influence of magnetic field, solidification [16], continuous casting of steel [17], and modelling of semiconductors [18] .

The thermomechanics model that is presented, is intended to complement the meshless model of mass and heat transfer, which is developed in our group [4]. In this contribution, first the meshless method formulation for solution of boundary value problem is given, followed by some method benchmarks on simple thermoelasticity problems. The thermoelasticity model is described and the preliminary results for stationary state of DC casting are presented.

2 GOVERNING EQUATION

We consider uncoupled formulation of thermoelasticity with stationary thermal profile supplied by the heat and mass transfer model. The stress equilibrium is written in terms of deformation field $\mathbf{u}$ by employing Hooke's law for an isotropic solid. Resulting governing equation is given as

$$G\nabla^2\mathbf{u}+(G+\lambda)\nabla\nabla\cdot\mathbf{u}+\nabla\lambda\nabla\cdot\mathbf{u}+\nabla G\left(\nabla\mathbf{u}+\left(\nabla\mathbf{u}\right)^T\right)=\nabla\left(\beta\left(T-T_{ref}\right)\right)-\mathbf{f}\,. \tag{1}$$

Here G stands for the shear modulus, λ for Lamé parameter and $\mathbf{f}$ for the body force. The coupling with the temperature field is described by the coefficient β defined as $\beta=(3\lambda+2G)\alpha$, where α is the coefficient of linear thermal expansion. T_{ref} stands for the reference temperature at which the thermal expansion is considered to be zero. All the material properties are allowed to vary over the computational domain in a continuous manner.

For the description of the problem setting, the displacement, symmetry, and traction boundary conditions are needed. The deformation of the top part of the billet is restricted by the mould, while the rest of the outer surface is free.

In the computational domain, the material undergoes solidification and therefore significantly changes the elastic properties. The temperature dependence of alloy properties can be obtained from JMatPro database for each alloy considered [19].

3 METHOD FORMULATION

The aim of our work is to develop a method to model the boundary value problem for linear vector partial differential equation (PDE) in two dimensions. The governing equation equation (1) can be written in the form $D_{\xi\zeta}u_{\zeta} = g_{\xi}$, with unknown solution vector u_{μ} and index μ running over the coordinates of the chosen coordinate system. The formulation of the method incorporates the following steps: construction of local influence domains, local interpolation, calculation of the differential operators, and the construction of the system of linear equations representing the governing PDE. These steps are described in the following subsections.

3.1 Node arrangement and influence domain selection

The first step is setting up an appropriate node arrangement and determining the domains of influence for each node. The determination of influence domains is especially important, since the local interpolation of the solution is constructed on them. In general N_{Γ} nodes are put on the boundary Γ and N_{Ω} are distributed over the interior Ω of the computational domain.

The node arrangement used in this work is obtained of by minimizing an energy function which is the sum of Lennard-Jones-like potentials among a certain number of nearby nodes as described in [20]. The procedure results in a node arrangement that is locally similar to the hexagonal grid and is illustrated Figure 1.

The domain of influence for each node is determined by choosing ${}_{l}N$ nearest neighbors of the node with index $l = 1,\ldots,N$, where $N = N_{\Gamma} + N_{\Omega}$ is the number of all discretization nodes. In this step we determine mapping $s_l(i) : i \to l'$ from the index $i = 1,...,{}_{l}N$, which enumerates the nodes in the local influence domain, to the global enumeration index l'.

3.2 Interpolant construction

Radial basis function (RBF) interpolant is constructed over each domain of influence. Modifed multiquadrics (MQ), defined as

$$\Phi_j(\mathbf{r}) = \sqrt{\left(\frac{\epsilon_l}{h_l}\right)^2 |\mathbf{r} - \mathbf{r}_j|^2 + 1}\,, \tag{2}$$

augmented by linear and constant monomials are selected. Quantities used in the MQ definition have the following meaning: $\mathbf{r}_j$ is the position of the node in which the MQ is centered, ϵ_l is the MQ shape parameter, which is allowed to be different for different influence domain, and h_l stands for the influence domain size defined as

$$h_l = \sqrt{\frac{\sum_{i=1}^{{}_{l}N} |\mathbf{r}_{s_l(i)} - \mathbf{r}_l|^2}{{}_{l}N - 1}} \tag{3}$$

Formally, the interpolant is given as

$$u_\xi(\mathbf{r}) = \sum_{i=1}^{{}_lN} {}_l\alpha_{i,\xi}\Phi_{s(i)}(\mathbf{r}) + \sum_{i={}_lN+1}^{{}_lN+{}_aN} {}_l\alpha_{i,\xi}p_i(\mathbf{r}-\mathbf{r}_l) = \sum_{i=1}^{{}_lN+{}_aN} {}_l\alpha_{i,\xi}\psi_i(\mathbf{r}) \tag{4}$$

where ${}_aN$ is the number of augmentation monomials used (in present work fixed to 3) and ${}_l\alpha_{i,\xi}$ are the expansion coefficients, which are determined by the collocation. The collocation equations, which are used to determine the coefficients ${}_l\alpha_{i,\xi}$ are modified so that the resulting interpolant satisfies the appropriate boundary conditions, if any of the nodes in the considered influence domain lies on the boundary. The system of equations obtained in this manner can be compactly written in matrix form as

$$\sum_{i,\zeta} {}_lA_{ji,\xi\zeta}\,{}_l\alpha_{i,\zeta} = {}_l\gamma_{j,\xi} \tag{5}$$

with the interpolation matrix ${}_lA$ and the right-hand side vector ${}_l\gamma$ given as

$${}_lA_{ji,\xi\chi} = \begin{cases} \Psi_i(\mathbf{r}_{{}_ls(j)})\delta_{\xi\chi} & \text{if } \mathbf{r}_{{}_ls(j)} \in \Omega \\ B_{\xi\chi}(\mathbf{r}_{{}_ls(j)})\Psi_i(\mathbf{r}_{{}_ls(j)}) & \text{if } \mathbf{r}_{{}_ls(j)} \in \Gamma \\ \mathrm{p}_j(\mathbf{r}_{{}_ls(\mathrm{i})})\delta_{\xi\chi} & \text{if } j > {}_lN \end{cases}, \tag{6}$$

$${}_l\gamma_{j,\xi} = \begin{cases} \mathrm{u}_\xi(\mathbf{r}_{{}_ls(j)}) & \text{if } \mathbf{r}_{{}_ls(j)} \in \Omega \\ b_\chi(\mathbf{r}_{{}_ls(j)}) & \text{if } \mathbf{r}_{{}_ls(j)} \in \Gamma \\ 0 & \text{if } j > {}_lN \end{cases}. \tag{7}$$

In the expressions (6) and (7) we assume that the boundary conditions are linear and specified by appropriate boundary condition operator as $B^j_{\xi\zeta}u_\zeta(\mathbf{r}_j) = b^j_\xi$.

3.3 Discretization of the governing equation

The interpolation of the field values specified in nodal points can be used to estimate the differential operators. Since the expansion coefficients are assumed to be constant, the differential operators act only on the basis functions. This fact can be used to discretize partial differential equations.

By replacing the unknown solution $\mathbf{u}$ with the interpolation given by equation (4), the governing equation at every interior node can be stated in terms of the interpolation coefficients. The interpolation coefficients are further replaced by the components of vector ${}_l\gamma$, thus expressing the governing equation at every interior node by the unknown solution values and given boundary conditions for nodes that belong to the influence domain, centered on the considered node. The resulting governing equation is for each interior node l stated as

$$\sum_{k,\chi} \Upsilon^{\Omega}_{{}_ls(k),\chi} u_{{}_ls(k),\chi} \sum_{i,\zeta} {}_lA^{-1}{}_{ik,\zeta\chi} D_{\xi\zeta}\psi_i(\mathbf{r}_l) = g_{l,\xi} - \sum_{k,\chi} \Upsilon^{\Gamma}_{{}_ls(k),\chi} b_{{}_ls(k),\chi} \sum_{i,\zeta} {}_lA^{-1}{}_{ik,\zeta\chi} D_{\xi\zeta}\psi_i(\mathbf{r}_l) \tag{8}$$

In this expression the boundary and the domain indicators Υ^{Γ}_j and Υ^{Ω}_j are used to achieve an efficient notation. The indicators evaluate to one, if the corresponding point j belongs to the set under consideration and to zero otherwise.

The set of linear equations for the unknown solution values stated in (8) is sparse and can be solved efficiently by specialized solvers. The numerical performance of the method has been investigated in our recent publications [21–23].

4 PRELIMINARY RESULTS ON LFEMC DC CASTING

4.1 Geometry and Boundary Conditions

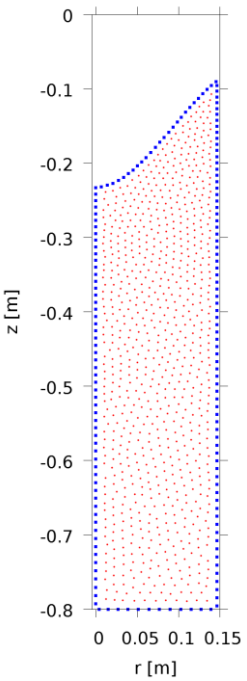

Figure 1 The node arrangement used for the discretization of the stress equilibrium equation. The circles represent interior points and the squares the boundary points.

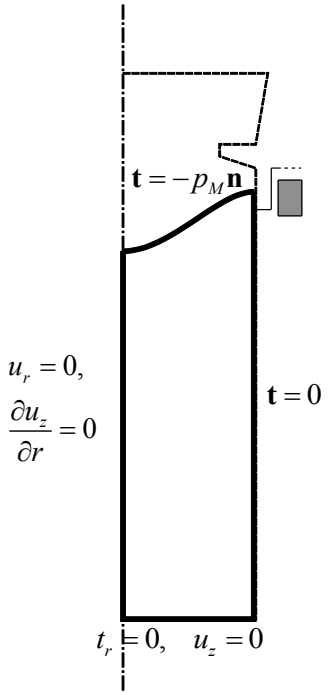

Figure 2 Geometry of the considered DC casting example with scheme of the boundary conditions. The computational domain for the solid mechanics model is denoted by solid line while the computational domain for the heat and mass transfer model additionally includes the part denoted by the dashed line.

In present work we are considering the governing equation (1) applied to the axisymmetric case of the DC casting of round aluminium billets. The temperature field, which has the largest influence on the deformation and stress field during DC casting, is calculated by the heat and fluid flow model. The model itself along with the material properties used is in more detail presented in the accompanying contribution by Šarler et al.. Material properties are obtained from the JMatPro for the alloy AA6082, which is being considered in our case.

Since linear thermoelasticity could not cope with the behavior of fluids, only the part of the billet that is solid is considered for the thermoelasticity model. The top boundary of the computational domain is chosen in such a way that it coincides with the position of the liquidus isotherm. The boundary conditions and the computational domain are shown in Figure 2. On the symmetry axis, the symmetry boundary conditions are assumed. On the bottom the deformation in vertical direction is assumed zero, while zero traction is prescribed in the radial direction. The outer surface is assumed to be free, except for the topmost part, which is constrained by the mould. In this part, the radial deformation is prescribed to be zero, while the zero traction is assumed in the vertical direction. On the top boundary, the

metallostatic pressure of the metal above the liquidus line is applied.

Although in DC casting many process parameters are important, in this work we are considering only the effect of low-frequency electromagnetic stirring (EMS). Some preliminary results regarding the effect of the two parameters are demonstrated in the following two sections. With the reference solution at nominal casting speed 80 mm/min and without the EMS applied is shown in Figure 3.

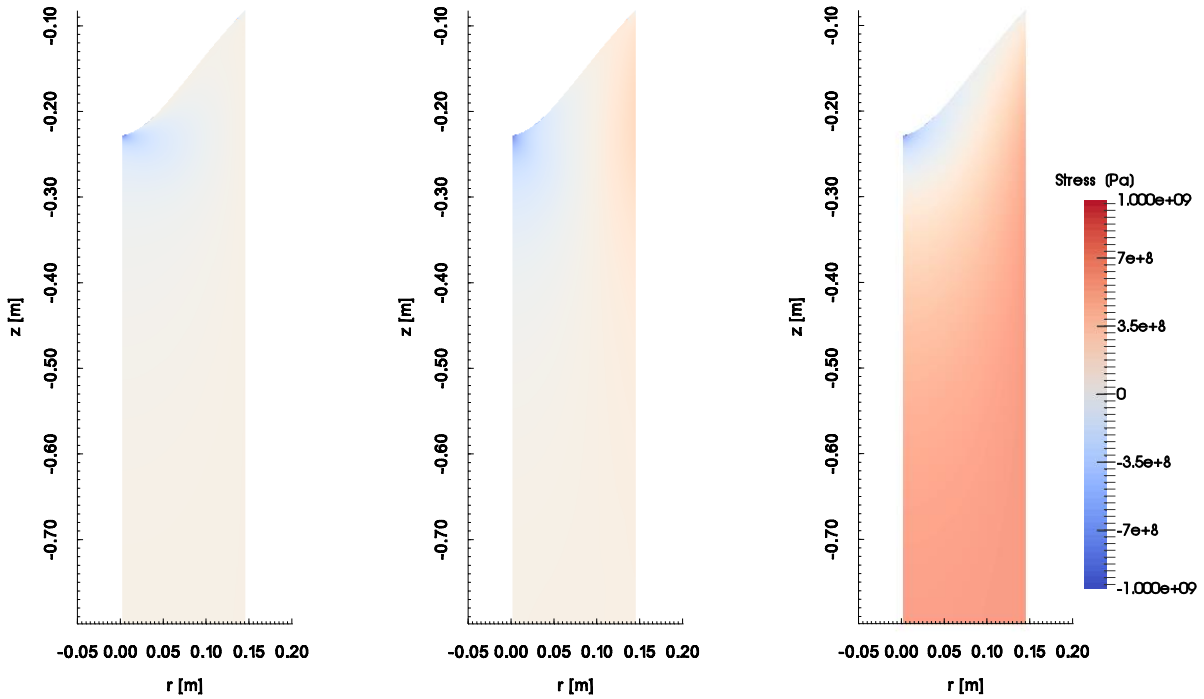

Figure 3 The stress state during DC casting. From left to right the plots show radial, vertical, and circumferential stress.

4.2 Effect of casting speed

Casting speed has important influence on the quality of the cast piece. The effect on the circumferential stress is shown in Figure 4. On all the plots the isoline of zero circumferential stress is shown. We can see that at the nominal casting speed of 80 mm/min the stress isoline touches the liquidus isoline on the surface of the billet. All the solidifying area thus experiences compressive stress. In case the casting speed is either increased or decreased, the zero stress isoline makes contact with the liquidus line in the interior of the billet. The solidifying area on the outside of the point of intersection experiences tensile stress, which increases the possibility of cracking.

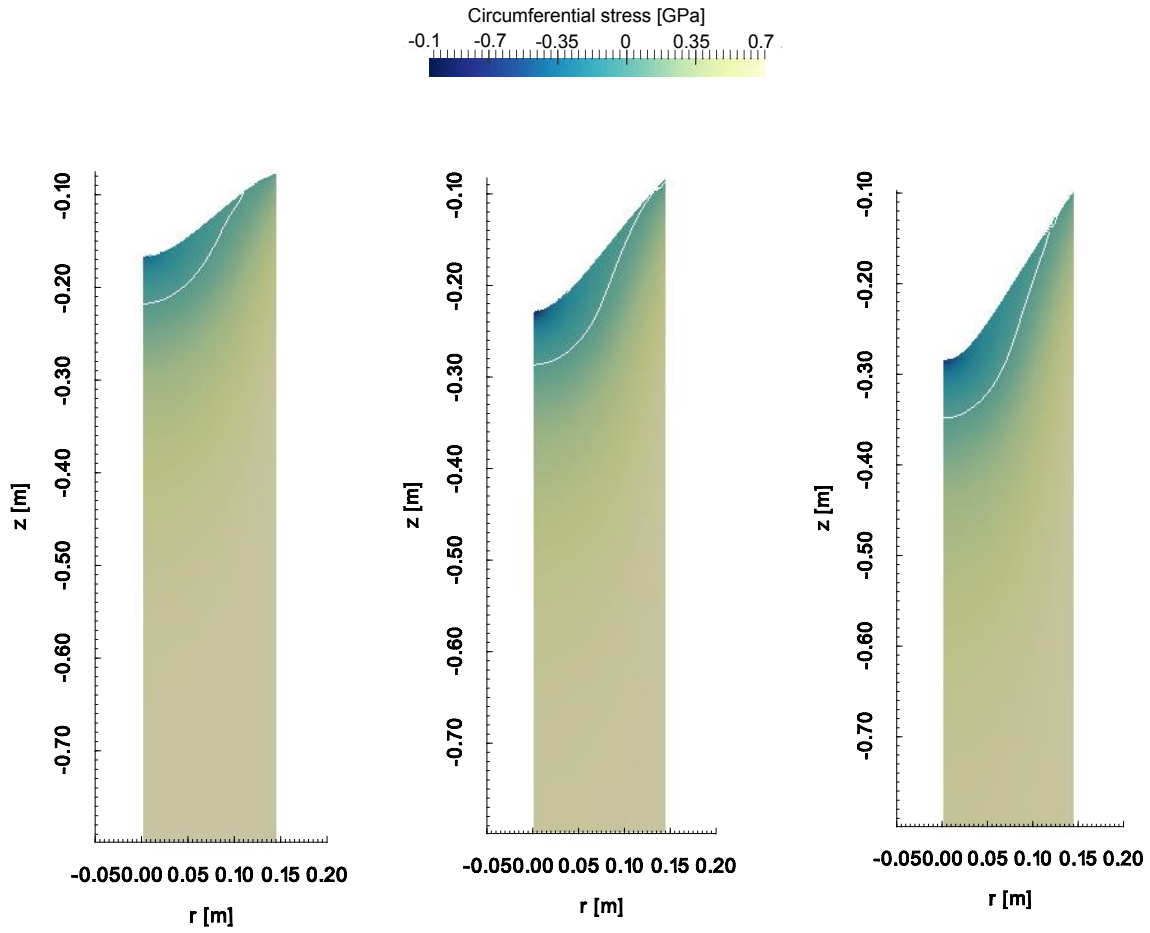

Figure 4 The effect of the casting speed on the circumferential stress. From left to right the plots show circumferential stress at casting speed of 60 mm/min, 80 mm/min and 100 mm/min. On each plot the zero isoline is shown.

4.3 Effect of EMS

In this study the driving current with amplitude 10 A and frequency 20 Hz has been applied to the casting process at the nominal casting speed of 80 mm/min. The difference between the reference stress without EMS and the stress when EMS is applied are shown in Figure 5. We can see that the application of EMS reduces the circumferential stress in the outer region and thus decreases the possibility of cracking. The effect of the EMS is beneficial also to the other two components, since the amplitude of the variations is slightly reduced.

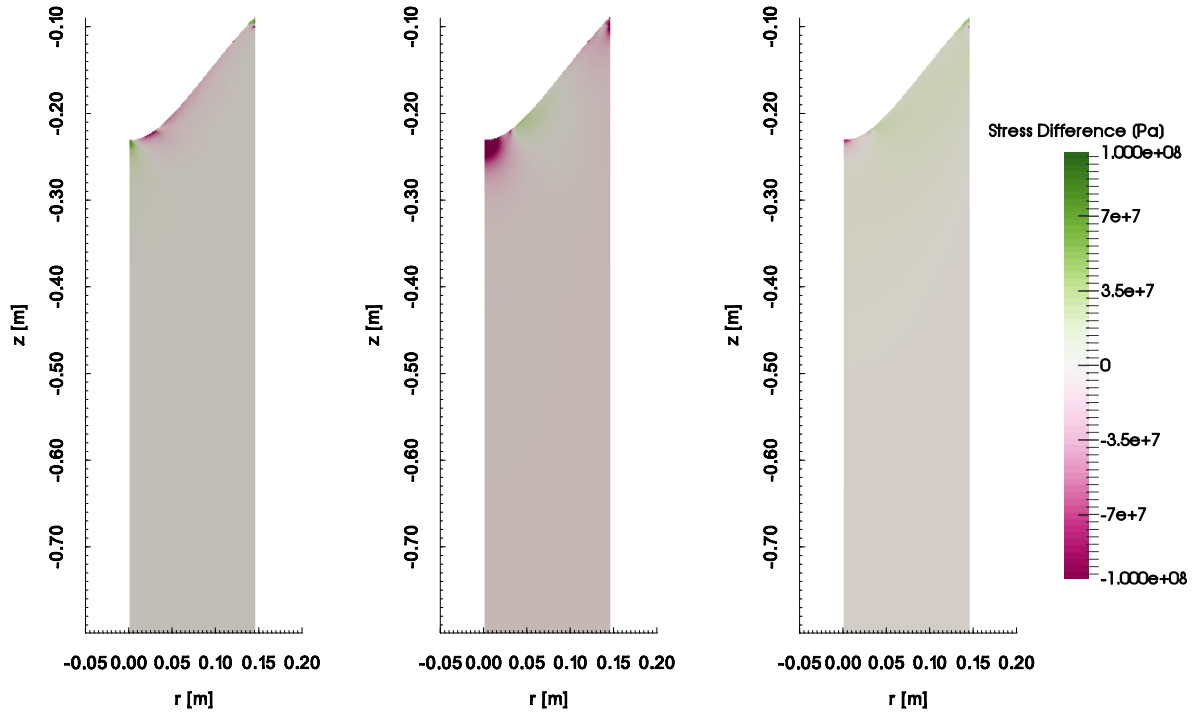

Figure 5 The difference in stress when the EMS is applied. From left to right the plots show the difference in radial, vertical, and circumferential stress.

5 CONCLUSIONS

The meshless method formulated in the paper is applied to the problem of LFEMC DC casting. The preliminary results obtained by the method show great potential in modelling of DC casting.

In this paper only a simple thermoelastic model for the stationary state of the process is considered. In the future, we plan on extending the model to incorporate plastic phenomena and to introduce full coupling between the deformation field and the heat and mass transfer model.

6 ACKNOWLEDGMENTS

Support from the Slovenian Grant Agency in the framework of the project L2-6775 and young researchers grants, Slovenian Ministry for Economy in the framework of the Voucher projects and IMPOL Aluminium Industry is kindly acknowledged.

REFERENCES

[1] Lalpoor, M. et al.: Cold cracking in DC-cast high strength aluminum alloy ingots: An intrinsic problem intensified by casting process parameters. *Mater. Sci. Eng. A*, **528** (6), 2011, p. 2831–2842.
[2] Eskin, D.G. *Physical Metallurgy of Direct Chill Casting of Aluminum Alloys*. Taylor & Francis, (2008).
[3] Fjaer, H.G., Mo, A. ALSPEN-A mathematical model for thermal stresses in direct chill casting of aluminum billets. *Metall. Trans. B* (1990) **21**:1049–1061.

[4] Drezet, J.M. et al. *Thermomechanical effects during direct chill and electromagnetic casting of aluminum alloys. Part II: numerical simulation*. TMS Publ., (1995).
[5] Kumar, P.P. et al. Mechanical Behavior of Mushy Zone in DC casting using a Viscoplastic Material Model. *Tech. Mech.* (2011) **32**:342–357.
[6] Zuo, Y. et al. Study on the sump and temperature field during low frequency electromagnetic casting a superhigh strength Al–Zn–Mg–Cu alloy. *J. Mater. Process. Technol.* (2008) **197:**109–115.
[7] Zhang, H., Cui, J. Production of super-high strength aluminum alloy billets by low frequency electromagnetic casting. *Trans. Nonferrous Met. Soc. China* (2011) **21:**2134–2139.
[8] Zhang, H. et al. Coupled modeling of electromagnetic field, fluid flow, heat transfer and solidification during low frequency electromagnetic casting of 7XXX aluminum alloys. *Mater. Sci. Eng. A* (2007) **448:** 189–203.
[9] M'Hamdi, M. et al. TearSim: A two-phase model addressing hot tearing formation during aluminum direct chill casting. *Metall. Mater. Trans. A* (2006) **37:**3069–3083.
[10] Nallathambi, A.K., Bertram, Albrecht, Specht, Eckehard et al. Thermomechanical simulation of direct chill casting. *Trans. Indian Inst. Met.* (2011) **64:**13–19.
[11] Liu, G.R. *Mesh Free Methods: Moving Beyond the Finite Element Method*. Taylor & Francis, (2010).
[12] Chen, Y. *Meshless methods in solid mechanics*. Springer, (2006).
[13] Kosec, G., Šarler, B. H-adaptive local radial basis function collocation meshless method. *Comput. Mater. Contin.*, (2011) **26:**227.
[14] Mramor, K. et al. Simulation of natural convection influenced by magnetic field with explicit local radial basis function collocation method. *CMES Comput. Model. Eng. Sci.* (2013) **92:**327–352.
[15] Vertnik, R., Šarler, B. Solution of incompressible turbulent flow by a mesh-free method. *Comput. Model. Eng. Sci. CMES* (2009) **44**:65.
[16] Kosec, G., Šarler, B.: Simulation of macrosegregation with mesosegregates in binary metallic casts by a meshless method. *Eng. Anal. Bound. Elem.* (2014) **45:**36–44.
[17] Vertnik, R.: *Heat and fluid flow simulation of the continuous casting of steel by a meshless method*. Nova Gorica: University of Nova Gorica, 2010.
[18] Kosec, G., Trobec, R.: Simulation of semiconductor devices with a local numerical approach. *Eng. Anal. Bound. Elem.* (2015) **50:**69–75.
[19] Saunders, N. et al.: Using JMatPro to model materials properties and behavior. *JOM* (2003) **55**:60–65.
[20] Košnik, N. et al.: Simulation of low frequency electromagnetic DC casting. *Mater. Sci. Forum* (2014) **790:**390–395.